
# Osteopontin expression in healing wounds of horses and in human keloids

| | |
|---|---|
| Journal: | *Equine Veterinary Journal* |
| Manuscript ID: | Draft |
| Wiley - Manuscript type: | General Article |
| Discipline: | Surgery general, Dermatology |
| Body System/Disorder: | Integument |
| Abstract: | Reasons for performing study<br>Osteopontin (OPN) is a matricellular protein involved in both physiological and pathological processes. Topical delivery of OPN antisense oligodeoxynucleotides resulted in accelerated healing and reduced granulation tissue formation and scarring in mice.<br>Objectives<br>Here we report OPN expression in an equine wound healing experimental model and in clinical specimens of equine exuberant granulation tissue (EGT) and human keloids.<br>Methods<br>OPN gene expression was evaluated by quantitative PCR while protein expression was investigated by mean of immunohistochemistry.<br>Results<br>q-PCR showed that OPN gene is constitutively expressed in normal intact skin of horses and continues to be expressed during the wound healing process. An increase in gene expression was observed at subsequent time points with a final decrease at wound closure. OPN protein was not detected in normal skin. Keratinocytes of wound edge samples did not express the protein. Dermal immunoreactivity was confined to inflammatory cells. Closed wounds were devoid of staining. Equine EGT showed immunoreactivity of epidermis, infiltrating neutrophils, mononuclear cells, endothelial cells and fibroblasts. Human keloids showed OPN immunoreactivity throughout epidermis as well as in mononuclear cells and scattered fibroblasts.<br>Conclusion<br>Our immunohistochemical data show a different pattern of expression between experimental and aberrant wounds thus suggesting a role in fibroproliferation in horses and humans. |
| | |

Abstract

**Reasons for performing study**

Osteopontin (OPN) is a matricellular protein involved in both physiological and pathological processes. Topical delivery of OPN antisense oligodeoxynucleotides resulted in accelerated healing and reduced granulation tissue formation and scarring in mice.

Objectives

Here we report OPN expression in an equine wound healing experimental model and in clinical specimens of equine exuberant granulation tissue (EGT) and human keloids.

**Methods**

OPN gene expression was evaluated by quantitative PCR while protein expression was investigated by mean of immunohistochemistry.

**Results**

q-PCR showed that OPN gene is constitutively expressed in normal intact skin of horses and continues to be expressed during the wound healing process. An increase in gene expression was observed at subsequent time points with a final decrease at wound closure. OPN protein was not detected in normal skin. Keratinocytes of wound edge samples did not express the protein. Dermal immunoreactivity was confined to inflammatory cells. Closed wounds were devoid of staining. Equine EGT showed immunoreactivity of epidermis, infiltrating neutrophils, mononuclear cells, endothelial cells and fibroblasts. Human keloids showed OPN immunoreactivity throughout epidermis as well as in mononuclear cells and scattered fibroblasts.

**Conclusion**

Our immunohistochemical data show a different pattern of expression between experimental and aberrant wounds thus suggesting a role in fibroproliferation in horses and humans.

## Introduction

Wounds located on the distal limb of horses exhibit persistent inflammation, greater retraction and premature cessation of contraction as well as slower rates of epithelialization[1]. Moreover, healing may be complicated by the formation of exuberant granulation tissue (EGT) that ultimately leads to exaggerated scarring[1]. Humans and horses are the only mammals known to naturally develop excessive fibroplasia during wound healing. While equine EGT is not epithelialized and possesses greater numbers of acute inflammatory cells, small vessels and myofibroblasts compared with keloids[2; 3], the two conditions are thought to share a similar pathogenesis.

It was recently confirmed that oxygen saturation values of limb wounds are inferior to those of body wounds during the early period of healing, indicating a temporary, relative state of hypoxia during the inflammatory phase of repair[4]. Interestingly, hypoxia has been proposed as a mechanism contributing to several human fibroproliferative disorders, including keloids[5; 6].

An hypoxic environment is able to reprogram the cytokine/chemokine expression profile, as documented in human mature dendritic cells[7], where, among hypoxia-inducible genes coding for cytokines with a primary role in inflammation and angiogenesis, Osteopontin (OPN) has been found to be upregulated more than vascular endothelial growth factor (VEGF) or interleukin (IL)-1β.

OPN null mice show defective debridement, greater disorganization of matrix and an alteration of collagen fibrillogenesis leading to small diameter collagen fibrils in healing skin wounds[8]. Moreover, in a mouse model of bleomycin-induced dermal fibrosis, OPN-deficient mice develop less fibrosis, coupled with reduced TGF-β1 levels, compared to wild type mice[9]. It thus appears that while OPN is essential to proper wound healing, a persistent or excessive expression will lead to fibrosis and superfluous scar formation. This hypothesis is further corroborated by Martin and collaborators[10], who investigated the effects of blocking OPN expression at the wound site in a series of *in vitro* and *in*

48 *vivo* studies based on the premise of inflammation-associated fibrosis. They demonstrated that
49 macrophage- and mast cell-secreted factors, specifically platelet-derived growth factor (PDGF), induce
50 fibroblast OPN expression in an *in vitro* setting. Moreover, by decreasing OPN protein levels in mouse
51 skin wounds via the topical delivery of OPN antisense oligodeoxynucleotides, they accelerated healing
52 and reduced granulation tissue formation and scarring.
53 Given the convincing evidence that persistent or excessive expression of OPN is linked to
54 fibroproliferation, the aim of the study presented herein was to investigate the OPN expression in an
55 equine wound healing model and in clinical specimens of equine EGT and human keloids.
56

## Methods

### Tissues, RNA extraction and cDNA synthesis

Normal intact skin samples from body, limb and bandaged limb, as well as wound edge samples, from same sites, collected at specific times during the repair process were obtained from four normal, 2- to 3-year-old Standardbred mares, as described[11]. Briefly, five 6.25 $cm^2$ areas were excised on the lateral thoracic wall (body) and on the dorso-lateral surface of one randomly assigned metacarpus beginning just above the fetlock (limb), 1.5 cm apart in a staggered vertical column, then left to heal by second intention. All horses had 1 randomly designated forelimb that was bandaged postoperatively with a nonadherent permeable dressing (Melolite; Smith-Nephew Canada, St-Lambert, Quebec). This was secured with 12-cm-wide sterile conforming gauze (Easifix; Smith-Nephew Canada) and then a cotton outer bandage, held in place with a 10-cm-wide rippable cohesive bandage (PowerFlex; Smith-Nephew Canada) and 1 turn of 7.6-cm-wide adhesive tape (Elastoplast; Smith-Nephew Canada) at either extremity, to induce the formation of exuberant granulation tissue and thus lead to scarring[12]. Bandages were changed every 2 to 3 d until complete healing.

Excised skin from the lowermost wound was kept as a time 0 sample (normal intact skin). One wound per site (body; limb and bandaged limb) was then sampled at the following times in each horse: 12h, 24h, 48h, 1 week and at wound closure. To avoid repeat trauma, each wound, beginning with the most distal/ventral one, was designated for a single biopsy.

These experiments were approved by the Animal Ethics Committee of the Faculté de Médecine Vétérinaire of the Université de Montréal and were sanctioned by the Canadian Council on Animal Care. Institutional approval for the ethical use of human samples was not needed since anonimous archival samples were used.

Full-thickness specimens were taken with an 8-mm diameter biopsy punch and divided in two halves, both including a 3- to 4-mm strip of peripheral skin, the migrating epithelium and a 3- to 4-mm strip of granulation tissue from the wound centre, when present. One half was snap-frozen in liquid nitrogen and stored at –80°C until total RNA was extracted with the RNeasy Fibrous Tissue Mini Kit following the manufacturer instructions (QIAGEN Inc. Ontario, CA). RNA was then analyzed by the NanoDrop 1000 Spectrophotometer (Thermo Fisher Scientific Inc., Waltham, MA, USA). Two µg of the extracted RNA was retro-transcribed using the SuperScript® VILO™ cDNA Synthesis Kit (11754-050, Invitrogen, Burlington, Ontario, Canada) according to the manufacturer's instructions, then stored at -80°C until use. The other half of the 8-mm diameter tissue section was processed for paraffin embedding.

Archival paraffin embedded samples of 3-month-old EGT located on the limb of three horses presented to the Centre Hospitalier Universitaire Vétérinaire of the Université de Montréal were obtained. Analogously, sections of human keloids were obtained from three clinical cases presented at the Division of Pathology, S. Andrea Hospital, La Spezia, Italy.

Tissue samples of equine kidney were obtained from a local slaughterhouse, immediately following evisceration, to provide positive controls for OPN immunodetection. Kidney specimens were either promptly frozen on dry ice for Western blot analysis or formalin fixed for paraffin embedding.

Paraffin sections were either stained for general morphology (Eosin-Haematoxylin, Mallory trichrome) or used for immunohistochemical evaluation of OPN immunoreactivity.

RT-PCR and qPCR

The gene expression in this study was assessed by two different methods. Conventional PCR was used as the appropriate method to determine primer specificity and the presence of splice variants. Samples

were obtained from normal intact skin and experimental wound edges (body and limbs pooled), sampled at 12, 24 and 48h post wounding. Total RNA was reverse transcribed using the SuperScript® ViloTM cDNA synthesis kit (mentioned above). Conventional PCR was performed with 1µL cDNA in a 25µL total volume with the Advantage 2 DNA polymerase kit (BD Biosciences Clontech). The following two sets of OPN primers were used: eOPN-F: 5'-CCA GTT AAT CAG GCC GAC TCT-3'; eOPN-R: 5'-TGG GCA CAG CTG GTG TAA AA-3'; eOPN-A: 5'-AGG CCG ACT CTG GCA GCT CT-3'; eOPN-1: 5'-TGG GGT TGC TGG AAC GTC GG-3'. Glyceraldehyde 3-phosphate dehydrogenase (GAPDH) was used as a housekeeping gene with the following primers: GAPDH-F: 5'-CAA GTT CCA TGG CAC AGT CAC GG-3'; GAPDH-R: 5'-AAA GTG GTC GTT GAG GGC AAT GC-3'. The 40 cycles reaction used to amplify each transcript included a thermal cycling parameter of 1 min at 94 °C, 30 sec at 63 °C and 1 min at 72 °C. The PCR product was resolved in a 2% agarose gel, using ethidium bromide as visualizing dye.

Following proper characterization of the amplicons by size of the bands, gene expression profile was assessed in cDNA from normal intact skin and experimental wound edges (sampled at 12h, 24h, 48h and 1 week post wounding as well as at wound closure) from body, limb and bandaged limbs by relative real-time PCR. Real-time PCR was conducted in an ABI Prism 7300 instrument in 25µl reaction volume containing 12.5µl of 2×Power SYBR Green PCR Master Mix (Applied Biosystems), 8.5µl of water, 2µl of each sample cDNA, eOPN-A and eOPN-1 (1µl each) as OPN primers. Beta-actin (ACTB) was used as a housekeeping gene (ACTB-F: 5'-CCG ACG GCC AGG TGA TC-3'; ACTB-R: 5'-TCG TGG ATA CCA CAA GAC TCC AT-3'). A common thermal cycling parameter (3 min at 95 °C, 40 cycles of 15 sec at 95 °C, 30 sec at 60 °C and 30 sec at 72 °C) was used to amplify each transcript. Identity of the amplicon was confirmed by sequencing. Melting curve analyses were routinely performed to verify product identity. Samples were run in duplicate and were expressed

relative to ACTB as housekeeping gene. Data were normalized to a calibrator sample (a mix of cDNA samples) using the ΔΔCt method with correction for amplification efficiency[13].

Statistical analysis: Gene-specific signals were normalized with corresponding ACTB signals for each sample. A repeated-measures linear model, with site and biopsy time as within-subject factors, was used to determine the effects of site and time on gene expression. *A priori* contrasts were performed to compare pairs of means and the comparisonwise alpha level was adjusted using Bonferroni's sequential adjustment procedure. The level of statistical significance was set at 0.05 and the statistical analyses were carried out with SAS version 9.3. (SAS Institute, Cary, NC, USA).

Western blot and Immunohistochemistry

Western blot (WB) analyses were performed on equine kidney extracts to confirm the specificity of the commercial mouse monoclonal anti-OPN antibody (sc-21742 - Santa Cruz Biotechnology – Santa Cruz CA) for equine tissues[14]. Briefly, 500 mg of horse kidney were homogenized in 5 mL of Laemmli solution by using gentleMACS™ Dissociator (MACS Miltenyi Biotec, Germany), according to the manufacturer's instructions. The homogenate was centrifuged and protein concentration was measured with a RC-DC Protein Assay from Bio-Rad using bovine serum albumin as the standard. Sample was stored at -80°C until analysis.

For Western blot, 30 µg of sample in Laemmli solution was run on 12% SDS-PAGE gel, then transferred onto nitrocellulose membranes (0.2 µm) using the Trans-Blot TurboTM (Biorad, Hercules, CA, USA) setting a voltage of 25V and an amperage of 1.3A for 7 minutes. Non-specific binding was prevented by blocking the membranes with 3% low fat dried milk, 0.2% (v/v) Tween 20 in PBS (10 mM $NaH_2PO_4$, pH 7.4, 0.9% NaCl) (PBS/milk/Tween) for 1 hr at room temperature. After blocking, the membranes were incubated with 1:200 anti-OPN antibody (mentioned above) in a blocking buffer

overnight at 4°C. After four washes with PBS/milk/Tween, the immunocomplexes were detected using a peroxidase-labelled secondary antibody (goat anti-mouse 1:10000 dilution, PerkinElmer Boston, MA USA). Immunoblots were developed using the ECL detection system. The chemiluminescent images were acquired by LAS4010 (GE Healthcare Europe GmbH, Milano, Italy). The experiment was performed in duplicate.

Immunohistochemistry was performed on normal intact skin, experimental wound edges and clinical samples of EGT from horses as well as human keloids; equine kidney served as a positive control. The peroxidase method with Diaminobenzidine as substrate was followed. Briefly, after Superfrost mounted 5 µm sections were rehydrated, epitope retrieval was carried out at 120°C in a pressure cooker for 5 minutes. Sections were then rinsed in PBS and incubated in 1% $H_2O_2$ in PBS for 10 minutes, then, to reduce non-specific staining, preincubated in PBS with 0.1% Triton X-100 (TX) (Sigma-Aldrich, St Louis, MO, USA) and in 5% normal horse serum (NS) (Vector Labs, Burlingame, CA). Next, sections were incubated overnight in a humid chamber at 4°C with the primary antibody (mentioned above, dilution 1:50) in PBS with 0.1% TX and 1% NS. After several washings in PBS, sections were incubated for 1 hour at room temperature in biotinylated horse anti-mouse immunoglobulin (Vector Labs, Burlingame, CA), diluted 1:300 in PBS. Sections were then washed for 3x10 minutes in PBS and incubated for 1 hour at room temperature in avidinbiotin-horseradish peroxidase complex (ABC; Vector Labs, Burlingame, CA), diluted 1:125 in PBS. After washing for 3x10 minutes in Tris/HCl (pH 7.6), peroxidase activity was detected by incubating in a solution of 0.125 mg/ml diaminobenzidine (Sigma-Aldrich, St. Louis, MO, USA) and 0.1% $H_2O_2$ in the same buffer for 10 minutes. The sections were examined and photographed with a light microscope (Leitz Diaplan, Leitz, Germany) equipped with a Nikon Digital Sight DS-U1 camera (Nikon Instruments S.p.A., Firenze, Italy).

172 Results

173 RT-PCR

174 Both sets of primers were specific against equine OPN. OPN gene was expressed in normal intact skin
175 and in wound edges (12, 24, 48 hours post wounding) of horses. A single band per sample was visible
176 thus confirming the absence of splice variants in normal intact skin and during the inflammatory phase
177 of equine wound healing (Figure 1). Blasting of the sequenced amplicons showed 100% identity with
178 the *Equus caballus* predicted sequence for transcript variant 1 (Gene bank accession number:
179 XM_001496152.2).

180

181 q-PCR

182 q-PCR showed that OPN gene is constitutively expressed in normal intact skin of horses and continues
183 to be expressed during the wound healing process (Figure 2). The overall trend was similar for all sites
184 (body, limb, bandaged limb) showing a rapid decrease of expression 12h post-wounding. An increase
185 in gene expression was however observed at subsequent time points (24h, 48h, 1 week) with a final
186 decrease at wound closure. No statistically significant differences were detected among wound sites;
187 differences between normal intact skin and wound edges were found only in the limb where the mean
188 at time 0 was significantly greater than at time 1 ($p = 0.0007$) but not at the subsequent time points.

189

190 Western blot and Immunohistochemistry

191 Western blot analyses conducted on equine kidney protein extracts to confirm the specificity of the
192 commercial antibody showed the presence of bands corresponding to data sheet information related to
193 OPN cleavage products: four bands of the estimated molecular weights of 60, 47, 37 and 31 kDa were

194 detected (not shown). Immunohistochemistry on equine kidney (positive control) showed immune-
195 reactivity in tubular cell cytoplasm while glomeruli remained devoid of staining (not shown).
196 OPN protein was not detected in normal skin in both the epidermal and the dermal compartment
197 (Figure 3b). Keratinocytes of wound edge samples did not express the protein throughout the
198 inflammatory phase (Figure 3c, e). Dermal immunoreactivity was observed from 12h post wounding
199 and consisted of staining of inflammatory cells, mainly neutrophils, at the wound edge (Figure 3d, f).
200 Samples taken at wound closure were devoid of staining.
201 Clinical samples of equine EGT stained for morphological evaluation (H&E and Mallory trichrome)
202 showed lack of epithelialization. Hyperplastic epidermis was visible at the edge of the lesion (Figure
203 4a). Scattered pigmented mononuclear cells were visible (Figure 4d). Acute inflammatory infiltrate was
204 present in the superficial portion of the specimen (Figure 4g). Immunohistochemical analysis showed
205 immunoreactivity of the basal portions of hyperplastic epidermis (Figure 4c). Infiltrating neutrophils as
206 well as endothelial cells and fibroblasts were immunoreactive to the OPN antibody (Figure 4i).
207 Mononuclear cells were strongly stained (Figure 4f).
208 Clinical samples of human keloids showed a moderately hyperplastic epidermis with a pigmented basal
209 layer (Figure 5a, b). The dermal compartment was characterized by the presence of keloidal collagen;
210 neutrophilic inflammatory infiltrate was absent (Figure 5d, e). OPN immunoreactivity was visible
211 throughout epidermis (Figure 5c) as well as in mononuclear cells and scattered fibroblasts (Figure 5f).
212
213

## Discussion

Before mapping the temporal pattern of OPN gene expression via quantitative PCR, we performed regular RT-PCR to investigate the presence of splice variants[15]. OPN has indeed been reported to exist as a full-length protein (OPN-a) and two splice variants (OPN-b, OPN-c). Seven exons are known to constitute the full length human OPN pre-mRNA[16] while OPN-b lacks exon 5 and OPN-c lacks exon 4[17-19]. On the basis of the *Equus caballus* predicted sequence for transcript variant 1 (XM_001496152.2) we selected two sets of primers flanking exons 4 and 5 in order to amplify eventual splice variants that were not found in horse skin. Although OPN alternative splicing has never been studied during wound healing, a number of studies of various cancer types suggest that OPN isoforms may have diverse effects and may be cancer type specific[20-26]. Results are conflicting and whether one isoform is most clinically relevant, or all three splice variants are important, remains unclear[15]. Since our amplicons perfectly aligned to *Equus caballus* predicted sequence for transcript variant 1 it is possible to deduce that the predicted full-length sequence (GeneBank accession number XM_001496152.2) is the only translated equine OPN in healing skin.

Besides, alternative splicing, post-translational modifications such as phosphorylation, glycosylation and proteolytic cleavage are reported for human OPN[15]. The latter may explain the detection of four bands of molecular weight lower than 60 kDa by WB analysis of equine kidney extracts. Both thrombin and MMPs are known to cleave human OPN and the aforementioned theoretical equine OPN shows one cleavage site for thrombin, two for MMP2 and twelve for MMP9. Further investigations, including full-length cloning and sequencing as well as biochemical characterization, are needed to better understand the properties of equine OPN and eventual analogies with its human counterpart.

The commercial antibody used in this study was assumed to be specific since, together with WB data, equine kidney showed the specific pattern of immunoreactivity (IHC) reported for humans[27].

Proteolytic cleavage of OPN precursor might also explain the discrepancy between the constitutive expression measured by PCR yet the absence of immunoreactivity in normal intact skin. On the basis of our data one can speculate that the commercial antibody does not recognize the precursor form of equine OPN that is constitutively transcribed but not cleaved in normal intact skin. Thrombin and MMPs are indeed present during the inflammatory phase of wound healing, which may lead to proteolysis with subsequent antigen retrieval.

A clear decrease in gene expression can be identified 12h post wounding with a subsequent rise at 24h in body wounds and at 48h in limb wounds. Although not statistically significant, the delay in restoration of OPN expression might recapitulate the delayed inflammatory response documented in experimental limb wounds when compared with body wounds in horses[28].

The only statistically significant difference between normal intact skin and wound edges was found in unbandaged limb wounds where the mean at time 0 was greater than at time 1. Such a difference was not found in bandaged limb wounds despite the trend was exactly the same.

Immunohistochemical staining of wounds showed immunoreactivity of the inflammatory infiltrate at the wound edge. OPN expression by inflammatory cells has been reported[15] and, as stated, the hypothesized role of OPN as a pro-fibrotic chemokine during wound healing is linked to the inflammatory phase[10]. Our quantitative gene expression and immunohistochemical data reflect the reported OPN up-regulation in association with the wound inflammatory response in mice[29].

Interestingly, the pattern of staining found in clinical samples of equine EGT and human keloid was distinct from that observed in the experimental wounds of horses. Hyperplastic epidermis flanking the periphery of non-epithelialized EGT lesions showed marked immunoreactivity of keratinocytes populating the basal portions. Similarly, human keloid keratinocytes were immunoreactive to OPN. While keratinocyte expression of OPN has been reported in squamous cell carcinoma in association

with malignancy in the form of invasion and metastasis[30; 31] as well as in chronic plaque psoriasis in association with the severity of disease[32], a role for keratinocyte expression of OPN in aberrant wound healing has never been reported.

The dermal compartment of EGT samples showed immunoreactivity of infiltrating neutrophils as well as endothelial cells and fibroblasts. Human keloid samples were devoid of acute inflammatory infiltrate and thus showed immunoreaction only of scattered fibroblasts.

Some mononucleated cells resembling macrophages appeared to be strongly stained in clinical samples of equine EGT. Their light brown staining in H&E section and also with the primary antibody omission suggests that the strong staining with the OPN antibody is not completely due to the presence of the protein. The brown pigment was confirmed to be hemosiderin (data not shown).

The staining of dermal fibroblasts mostly found in EGT but also in keloid samples, was not found in fibroblasts populating experimental wounds. The stronger immunoreactivity of EGT to OPN may be related to the greater number of fibroblasts but also to the accrued presence of myofibroblasts. OPN expression is indeed required for myofibroblast differentiation[33] and EGT was recently shown to possess markedly increased numbers of myofibroblasts compared with keloids[2].

Further investigations, including the possible down-regulation of OPN expression during equine experimental wound healing, as already performed in mice[10] may lead to the development of a novel therapeutic option for both equine EGT and human keloids, dermal fibroproliferative disorders that have yet to be resolved in a successful fashion.

Acknowledgements

Authors wish to acknowledge Gustavo Zamberlam, Christopher Price, Derek Boerboom and Alexandre Boyer for their technical assistance, Guy Beauchamp for statistical analysis and Nader Gorji for providing human keloid samples.

## References


[1] Hendrickson, D. and Virgin, J. (2005) Factors that affect equine wound repair. *The Veterinary clinics of North America. Equine practice* **21**, 33-44.

[2] Theoret, C.L., Olutoye, O.O., Parnell, L.K. and Hicks, J. (2013) Equine exuberant granulation tissue and human keloids: A comparative histopathologic study. *Veterinary surgery : VS*.

[3] Theoret, C.L. and Wilmink, J.M. (2013) Aberrant wound healing in the horse: naturally occurring conditions reminiscent of those observed in man. *Wound repair and regeneration : official publication of the Wound Healing Society [and] the European Tissue Repair Society* **21**, 365-371.

[4] Celeste, C.J., Deschene, K., Riley, C.B. and Theoret, C.L. (2011) Regional differences in wound oxygenation during normal healing in an equine model of cutaneous fibroproliferative disorder. *Wound repair and regeneration : official publication of the Wound Healing Society [and] the European Tissue Repair Society* **19**, 89-97.

[5] Kischer, C.W. (1992) The microvessels in hypertrophic scars, keloids and related lesions: a review. *Journal of submicroscopic cytology and pathology* **24**, 281-296.

[6] Zhang, Q., Oh, C.K., Messadi, D.V., Duong, H.S., Kelly, A.P., Soo, C., Wang, L. and Le, A.D. (2006) Hypoxia-induced HIF-1 alpha accumulation is augmented in a co-culture of keloid fibroblasts and human mast cells: involvement of ERK1/2 and PI-3K/Akt. *Experimental cell research* **312**, 145-155.

[7] Blengio, F., Raggi, F., Pierobon, D., Cappello, P., Eva, A., Giovarelli, M., Varesio, L. and Bosco, M.C. (2013) The hypoxic environment reprograms the cytokine/chemokine expression profile of human mature dendritic cells. *Immunobiology* **218**, 76-89.

[8] Liaw, L., Birk, D.E., Ballas, C.B., Whitsitt, J.S., Davidson, J.M. and Hogan, B.L. (1998) Altered wound healing in mice lacking a functional osteopontin gene (spp1). *The Journal of clinical investigation* **101**, 1468-1478.

[9] Wu, M., Schneider, D.J., Mayes, M.D., Assassi, S., Arnett, F.C., Tan, F.K., Blackburn, M.R. and Agarwal, S.K. (2012) Osteopontin in systemic sclerosis and its role in dermal fibrosis. *The Journal of investigative dermatology* **132**, 1605-1614.

[10] Mori, R., Shaw, T.J. and Martin, P. (2008) Molecular mechanisms linking wound inflammation and fibrosis: knockdown of osteopontin leads to rapid repair and reduced scarring. *The Journal of experimental medicine* **205**, 43-51.

[11] Lepault, E., Celeste, C., Dore, M., Martineau, D. and Theoret, C.L. (2005) Comparative study on microvascular occlusion and apoptosis in body and limb wounds in the horse. *Wound repair and regeneration : official publication of the Wound Healing Society [and] the European Tissue Repair Society* **13**, 520-529.

[12] Theoret, C.L., Barber, S.M., Moyana, T.N. and Gordon, J.R. (2002) Preliminary observations on expression of transforming growth factors beta1 and beta3 in equine full-thickness skin wounds healing normally or with exuberant granulation tissue. *Veterinary surgery : VS* **31**, 266-273.

[13] Pfaffl, M.W. (2001) A new mathematical model for relative quantification in real-time RT-PCR. *Nucleic acids research* **29**, e45.

[14] Xie, Y., Sakatsume, M., Nishi, S., Narita, I., Arakawa, M. and Gejyo, F. (2001) Expression, roles, receptors, and regulation of osteopontin in the kidney. *Kidney international* **60**, 1645-1657.

[15] Anborgh, P.H., Mutrie, J.C., Tuck, A.B. and Chambers, A.F. (2011) Pre- and post-translational regulation of osteopontin in cancer. *Journal of cell communication and signaling* **5**, 111-122.

[16] Rodrigues, L.R., Teixeira, J.A., Schmitt, F.L., Paulsson, M. and Lindmark-Mansson, H. (2007) The role of osteopontin in tumor progression and metastasis in breast cancer. *Cancer epidemiology, biomarkers & prevention : a publication of the American Association for Cancer Research, cosponsored by the American Society of Preventive Oncology* **16**, 1087-1097.

[17] Kiefer, M.C., Bauer, D.M. and Barr, P.J. (1989) The cDNA and derived amino acid sequence for human osteopontin. *Nucleic acids research* **17**, 3306.

[18] Young, M.F., Kerr, J.M., Termine, J.D., Wewer, U.M., Wang, M.G., McBride, O.W. and Fisher, L.W. (1990) cDNA cloning, mRNA distribution and heterogeneity, chromosomal location, and RFLP analysis of human osteopontin (OPN). *Genomics* **7**, 491-502.

[19] Hijiya, N., Setoguchi, M., Matsuura, K., Higuchi, Y., Akizuki, S. and Yamamoto, S. (1994) Cloning and characterization of the human osteopontin gene and its promoter. *The Biochemical journal* **303 ( Pt 1)**, 255-262.

[20] He, B., Mirza, M. and Weber, G.F. (2006) An osteopontin splice variant induces anchorage independence in human breast cancer cells. *Oncogene* **25**, 2192-2202.

[21] Mirza, M., Shaughnessy, E., Hurley, J.K., Vanpatten, K.A., Pestano, G.A., He, B. and Weber, G.F. (2008) Osteopontin-c is a selective marker of breast cancer. *International journal of cancer. Journal international du cancer* **122**, 889-897.

[22] Chae, S., Jun, H.O., Lee, E.G., Yang, S.J., Lee, D.C., Jung, J.K., Park, K.C., Yeom, Y.I. and Kim, K.W. (2009) Osteopontin splice variants differentially modulate the migratory activity of hepatocellular carcinoma cell lines. *International journal of oncology* **35**, 1409-1416.

[23] Ivanov, S.V., Ivanova, A.V., Goparaju, C.M., Chen, Y., Beck, A. and Pass, H.I. (2009) Tumorigenic properties of alternative osteopontin isoforms in mesothelioma. *Biochemical and biophysical research communications* **382**, 514-518.

[24] Sullivan, J., Blair, L., Alnajar, A., Aziz, T., Ng, C.Y., Chipitsyna, G., Gong, Q., Witkiewicz, A., Weber, G.F., Denhardt, D.T., Yeo, C.J. and Arafat, H.A. (2009) Expression of a prometastatic splice variant of osteopontin, OPNC, in human pancreatic ductal adenocarcinoma. *Surgery* **146**, 232-240.

[25] Yan, W., Qian, C., Zhao, P., Zhang, J., Shi, L., Qian, J., Liu, N., Fu, Z., Kang, C., Pu, P. and You, Y. (2010) Expression pattern of osteopontin splice variants and its functions on cell apoptosis and invasion in glioma cells. *Neuro-oncology* **12**, 765-775.

[26] Goparaju, C.M., Pass, H.I., Blasberg, J.D., Hirsch, N. and Donington, J.S. (2010) Functional heterogeneity of osteopontin isoforms in non-small cell lung cancer. *Journal of thoracic oncology : official publication of the International Association for the Study of Lung Cancer* **5**, 1516-1523.

[27] Hudkins, K.L., Giachelli, C.M., Cui, Y., Couser, W.G., Johnson, R.J. and Alpers, C.E. (1999) Osteopontin expression in fetal and mature human kidney. *Journal of the American Society of Nephrology : JASN* **10**, 444-457.

[28] Wilmink, J.M., van Weeren, P.R., Stolk, P.W., Van Mil, F.N. and Barneveld, A. (1999) Differences in second-intention wound healing between horses and ponies: histological aspects. *Equine veterinary journal* **31**, 61-67.

[29] Cooper, L., Johnson, C., Burslem, F. and Martin, P. (2005) Wound healing and inflammation genes revealed by array analysis of 'macrophageless' PU.1 null mice. *Genome biology* **6**, R5.

[30] Routray, S., Kheur, S.M. and Kheur, M. (2013) Osteopontin: a marker for invasive oral squamous cell carcinoma but not for potentially malignant epithelial dysplasias. *Annals of Diagnostic Pathology* **17**, 421-424.

[31] Chang, P.L., Harkins, L., Hsieh, Y.H., Hicks, P., Sappayatosok, K., Yodsanga, S., Swasdison, S., Chambers, A.F., Elmets, C.A. and Ho, K.J. (2008) Osteopontin expression in normal skin and non-melanoma skin tumors. *The journal of histochemistry and cytochemistry : official journal of the Histochemistry Society* **56**, 57-66.

[32] Abdou, A.G., El Farargy, S., Seleit, I., Antar, A.G., Elhefny, M. and Elnaidany, N.F. (2012) Osteopontin expression in chronic plaque psoriasis: an association with the severity of disease. *Analytical and quantitative cytology and histology / the International Academy of Cytology [and] American Society of Cytology* **34**, 79-85.

[33] Lenga, Y., Koh, A., Perera, A.S., McCulloch, C.A., Sodek, J. and Zohar, R. (2008) Osteopontin expression is required for myofibroblast differentiation. *Circulation research* **102**, 319-327.

Figure Legends

Figure 1: PCR data. A single splice variant was present during the inflammatory phase of experimental wound healing in horses.

Figure 2: qPCR data. *= statistically different to normal intact skin

Figure 3: OPN expression in experimental equine wound healing: a) H&E stained normal intact skin. b) OPN is not detected in normal intact skin; c, e) wound edge 12 h and 48 h post wounding focusing on epidermis, OPN is not present; d, f) wound edge 12 h and 48 h post wounding focusing on dermis, OPN is present in the inflammatory infiltrate. Scale bar = 50 µm.

Figure 4: a) H&E stained equine EGT focusing on the epidermal compartment; b) primary antibody omission; c) OPN immunostaining showing strong epidermal reactivity at the periphery of the lesion (arrowheads); d) H&E stained equine EGT focusing on the dermal compartment; e) primary antibody omission: the stained mononuclear cells might represent macrophages with either melanin or ferritin phagosomes; f) OPN immunohistochemistry with strong staining of mononuclear cells analogous to (e); g) H&E stained equine EGT focusing on the acute inflammatory infiltrate (neutrophils); h) OPN immunoreactivity of neutrophils; i) OPN immunoreactivity of fibroblasts (asterisks) and endothelium (arrowhead). Scale bars: a-c = 200 µm; d-i = 50 µm.

Figure 5: a) Mallory stained human keloid focusing on the epidermal compartment; b) same as (a), H&E stained; c) OPN immunostaining showing epidermal reactivity; basal staining mostly due to

presence of melanin; d) Mallory stained human keloid focusing on the dermal compartment; e) same as (d), H&E stained; f) Mononuclear cells and scattered fibroblasts immunoreactive to OPN. Scale bars: a-e= 50 µm; f = 80 µm.

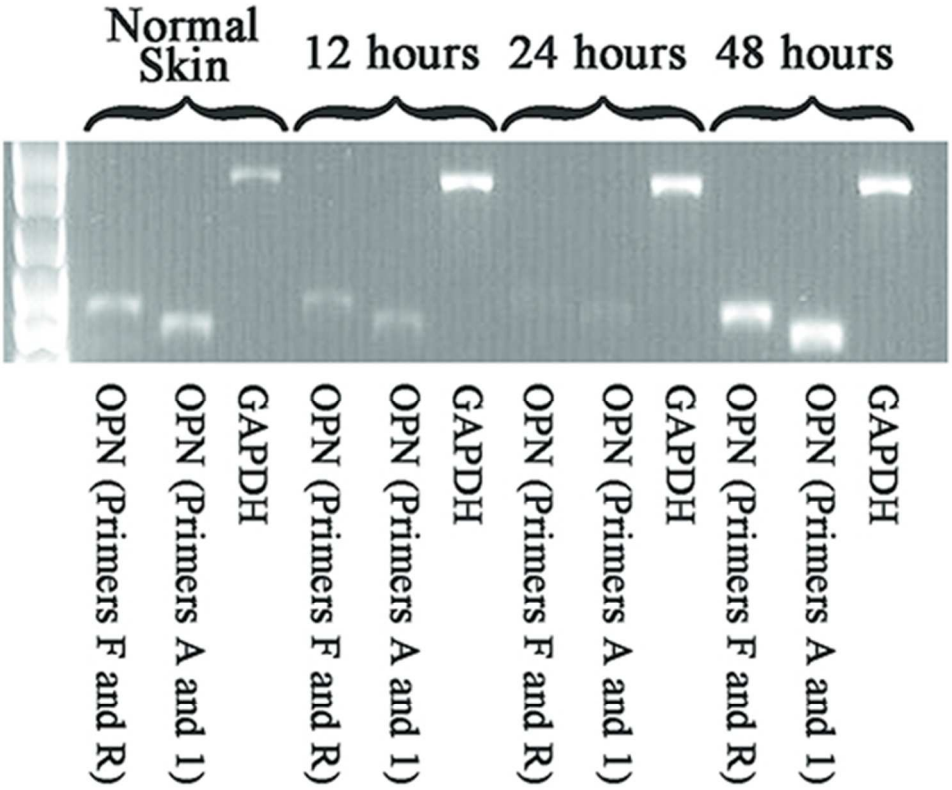


PCR data. A single splice variant was present during the inflammatory phase of experimental wound healing in horses.
43x35mm (300 x 300 DPI)

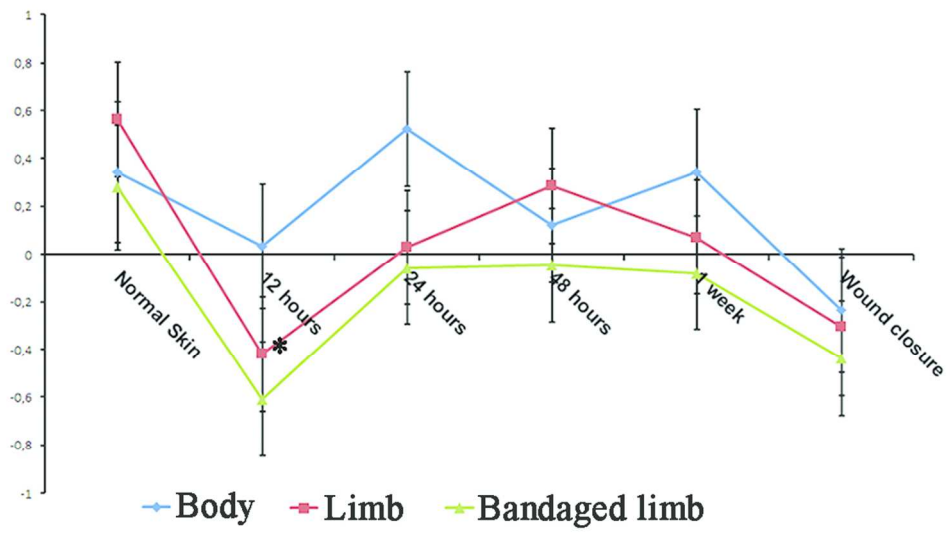


qPCR data. *= statistically different to normal intact skin
99x55mm (300 x 300 DPI)

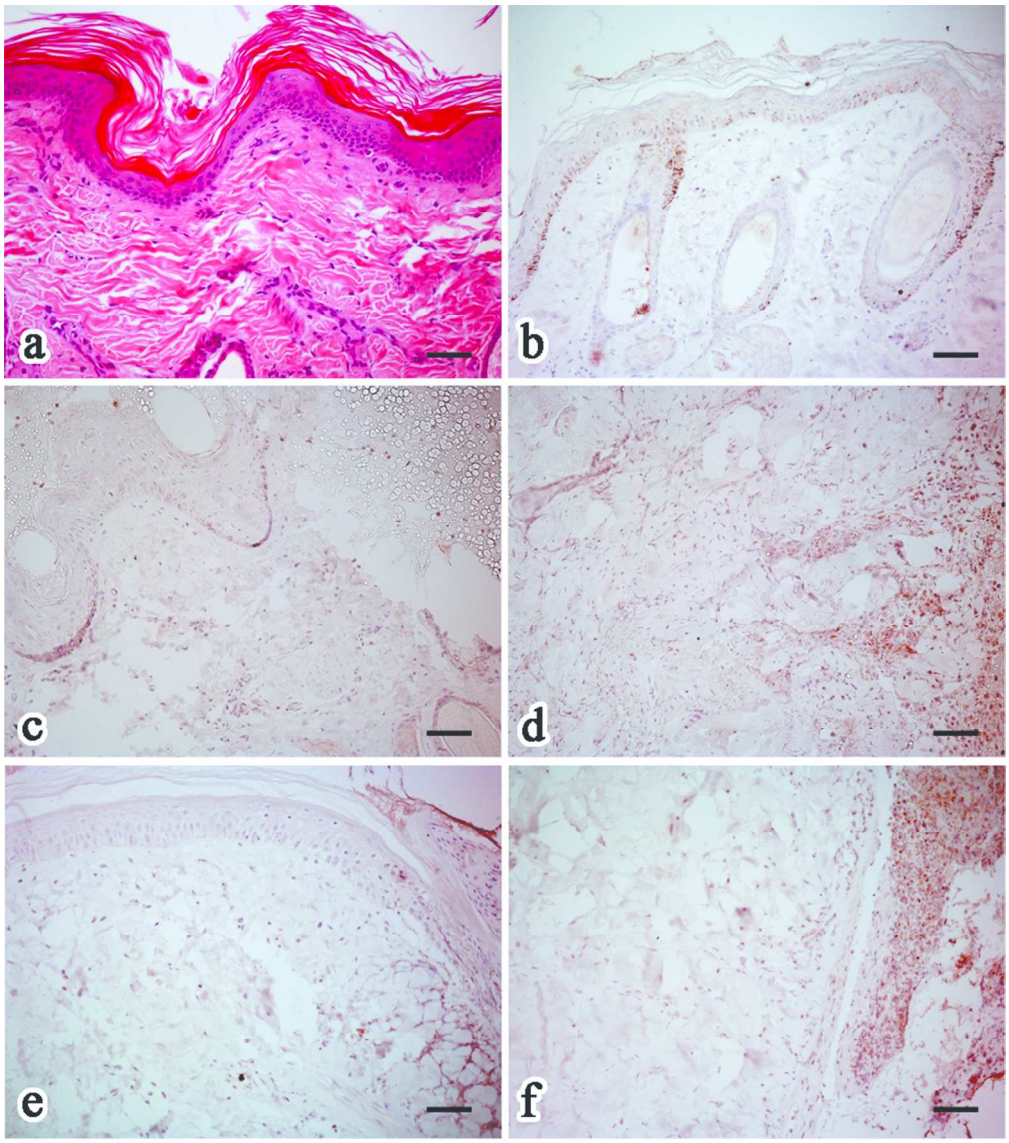


OPN expression in experimental equine wound healing: a) H&E stained normal intact skin. b) OPN is not detected in normal intact skin; c, e) wound edge 12 h and 48 h post wounding focusing on epidermis, OPN is not present; d, f) wound edge 12 h and 48 h post wounding focusing on dermis, OPN is present in the inflammatory infiltrate. Scale bar = 50 μm.
143x162mm (300 x 300 DPI)

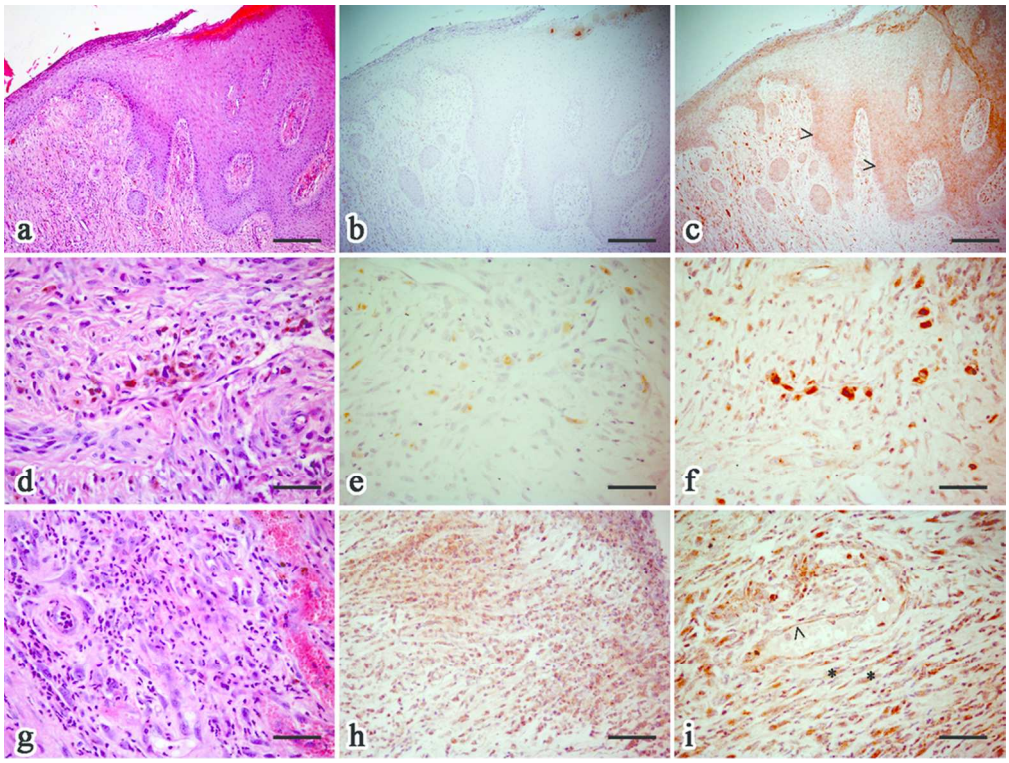


a) H&E stained equine EGT focusing on the epidermal compartment; b) primary antibody omission; c) OPN immunostaining showing strong epidermal reactivity at the periphery of the lesion (arrowheads); d) H&E stained equine EGT focusing on the dermal compartment; e) primary antibody omission: the stained mononuclear cells might represent macrophages with either melanin or ferritin phagosomes; f) OPN immunohistochemistry with strong staining of mononuclear cells analogous to (e); g) H&E stained equine EGT focusing on the acute inflammatory infiltrate (neutrophils); h) OPN immunoreactivity of neutrophils; i) OPN immunoreactivity of fibroblasts (asterisks) and endothelium (arrowhead). Scale bars: a-c = 200 µm; d-i = 50 µm.
95x71mm (300 x 300 DPI)

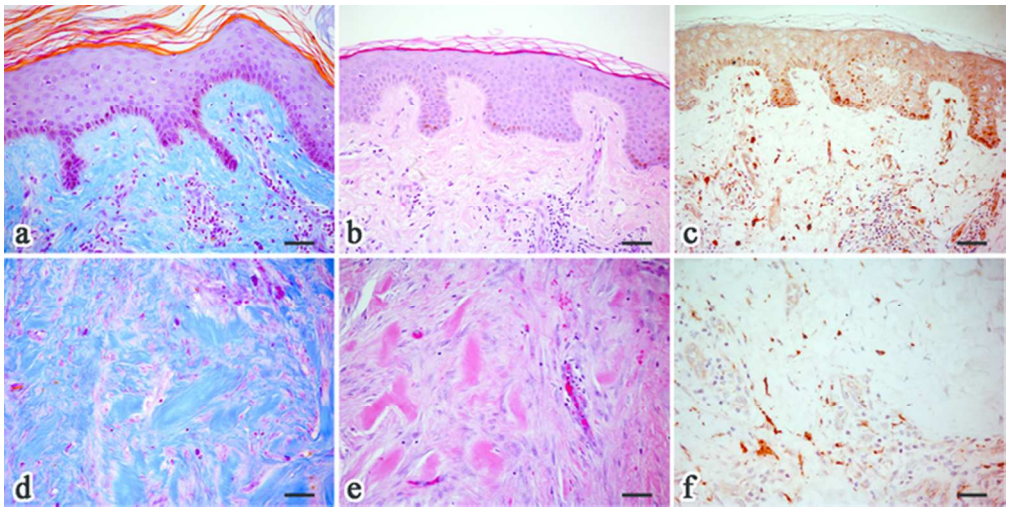


a) Mallory stained human keloid focusing on the epidermal compartment; b) same as (a), H&E stained; c) OPN immunostaining showing epidermal reactivity; basal staining mostly due to presence of melanin; d) Mallory stained human keloid focusing on the dermal compartment; e) same as (d), H&E stained; f) Mononuclear cells and scattered fibroblasts immunoreactive to OPN. Scale bars: a-e= 50 µm; f = 80 µm.
63x31mm (300 x 300 DPI)